Acoustic trapping based on surface displacement of resonance modes[a]

Björn Hammarström,[1,b] Nils R. Skov,[2] Karl Olofsson,[1,c] Henrik Bruus,[2,d] and Martin Wiklund[1,e]

[1]*Department of Applied Physics, KTH Royal Institute of Technology, Roslagstullsbacken 21, SE-114 21 Stockholm, Sweden*

[2]*Department of Physics, Technical University of Denmark, DTU Physics Building 309, DK-2800 Kongens Lyngby, Denmark*

ABSTRACT:

Acoustic trapping is a promising technique for aligning particles in two-dimensional arrays, as well as for dynamic manipulation of particles individually or in groups. The actuating principles used in current systems rely on either cavity modes in enclosures or complex arrangements for phase control. Therefore, available systems either require high power inputs and costly peripheral equipment or sacrifice flexibility. This work presents a different concept for acoustic trapping of particles and cells that enables dynamically defined trapping patterns inside a simple and inexpensive setup. Here, dynamic operation and dexterous trapping are realized through the use of a modified piezoelectric transducer in direct contact with the liquid sample. Physical modeling shows how the transducer induces an acoustic force potential where the conventional trapping in the axial direction is supplemented by surface displacement dependent lateral trapping. The lateral field is a horizontal array of pronounced potential minima with frequency-dependent locations. The resulting system enables dynamic arraying of levitated trapping sites at low power and can be manufactured at ultra-low cost, operated using low-cost electronics, and assembled in less than 5 min. We demonstrate dynamic patterning of particles and biological cells and exemplify potential uses of the technique for cell-based sample preparation and cell culture. © *2021 Acoustical Society of America.*
https://doi.org/10.1121/10.0003600

I. INTRODUCTION

Acoustic trapping has been applied in a wide range of applications in life sciences, ranging from diagnostics, automation of laboratory tasks, and sample preparation and separation (Clark *et al.*, 2019; Hammarström *et al.*, 2014a; Ohlsson *et al.*, 2018) to the creation of better biological model systems and tissue engineering (Bouyer *et al.*, 2016). Ultrasound-based methods have proven to be a gentle way of handling (Olofsson *et al.*, 2018) as compared to alternative external field methods, such as optical trapping (Jing *et al.*, 2016) and dielectrophoresis (Md Ali *et al.*, 2018; Voldman, 2006), which require careful consideration in order not to induce cell damage. Acoustic manipulation generally does not alter cell functionality, and standing waves can be applied onto large cell populations over extended periods of time without noticeable loss of cell viability (Burguillos *et al.*, 2013; Hultström *et al.*, 2007); it can therefore be used to build advanced model systems (Christakou *et al.*, 2015; Jonnalagadda *et al.*, 2018; Tait *et al.*, 2019; Takebe and Wells, 2019).

From a technology perspective, tremendous improvements in the dexterity and precision of acoustic traps, or tweezers, have been achieved in recent years. By utilizing multiple piezoelectric elements in precisely controlled arrangements, highly regular three-dimensional (3D) particle patterns have been demonstrated (Caleap and Drinkwater, 2014), and phase-controlled excitation of transducer elements (Courtney *et al.*, 2013) has extended the ability to move the particles in collective patterns and individually (Marzo *et al.*, 2015). As an alternative to large transducer arrays, the inclusion of holographic phase-plates in order to generate generic but predefined trapping fields has been suggested (Melde *et al.*, 2016). For single cell manipulation, Baudoin *et al.* (2019) introduced a transducer geometry capable of forming a focalized vortex with a single trapping site. By moving the transducer laterally, they demonstrated the ability to drag a single particle located in the focal spot. While these developments promise to significantly improve the capabilities of acoustic trapping, translation of these novel and more flexible trapping technologies to applications in cell handling on a larger scale, such as sample preparation and studies of biological systems, is yet to be seen for several reasons.

One of the main obstacles when using acoustic trapping is the voltages needed to drive the piezo at a sufficient displacement amplitude to reach the required radiation force amplitudes in the liquid. To drive the piezo at these voltages, an amplifier is usually needed, which limits the possibilities for device parallelization. Due to losses in the electric and mechanical transduction, the voltages might

---

[a]This paper is part of a special issue on Theory and Applications of Acoustofluidics.
[b]Electronic mail: bham@kth.se, ORCID: 0000-0002-3422-1325.
[c]ORCID: 0000-0002-3976-3430.
[d]ORCID: 0000-0001-5827-2939.
[e]ORCID: 0000-0002-3247-1945.

also introduce a significant heat source, which has to be counteracted with a heat sink, thus extending the surrounding equipment required to operate an acoustic trap. For emerging acoustofluidic technologies aiming at low-cost sample preparation or the study of complex biological systems, a high degree of robustness and parallelization is imperative. Two suggested approaches based on ultrasound are to either implement parallelization within a single device through the formation of a grid or array of trapped cells (Chen *et al.*, 2016; Christakou *et al.*, 2015) or to adopt a minimalistic low-cost system where several devices can be operated simultaneously, as exemplified by the trapping capillaries (Hammarström *et al.*, 2014b).

The main novelty of the acoustic trapping system described in this paper is the technology based on surface displacement of bulk resonance modes in the piezoelectric transducer (PZT). The proposed arrangement uses an optimized single-axis ultrasonic PZT to effectively feed large amounts of acoustic energy into the fluid sample containing cells or particles. Subsequently, we show that the lateral distribution of this energy in the fluid is determined solely by the surface displacement of specific 3D resonance modes in the attached piezoelectric element (called PZT modes in the following) instead of the conventional method where the acoustic energy distribution is determined by 3D cavity modes defined by a fluid-filled enclosure (Hagsäter *et al.*, 2008), and eventually by a complex 3D system resonance including all solid parts of the device in contact with this enclosure (Skov *et al.*, 2019). Through a predictive design of a single element piezo, these specific PZT modes allow the 3D shape of the acoustic field and thus the acoustic trapping potential to be dynamically controlled by the electrical driving parameters. Sustaining lateral manipulation through this mechanism turns out to be a highly energy efficient approach, and manipulation at sub-milliwatt power levels is made possible. The low-power operation enables the demonstration of a battery powered acoustic trap using inexpensive digital electronics at a cost several orders of magnitude lower compared to conventional micro-scaled acoustic traps driven by amplifiers costing more than 10 000 euros. In combination with the straightforward device design, a truly fast-to-manufacture and low-cost strategy also at a system level is achieved.

The ability of temporal control and flow-free transport of particles is demonstrated through different actuation schemes, and we showcase the ability to robustly retain the levitated aggregates against fluid flows and gas pocket disturbances. Last, the potential of the technology in sample preparation and cell handling applications is showcased by preforming medium exchange around levitated particles and two-dimensional (2D) arraying of captured cell aggregates.

II. RESULTS

A. Device model

The combination of a 2 MHz piezo, a 390-μm-thick fluid layer, and a glass reflector is expected to produce a

highly efficient *layered-resonator*, as described by Glynne-Jones *et al.* (2012). Utilizing a model originally proposed by Krimholtz *et al.* (1970), i.e., the KLM-model, the study of Glynne-Jones *et al.* suggests that the fundamental resonance of such a system will occur around 1.8 MHz and produces a single pressure-minimum (and thus a single force-potential minimum) in the fluid.

In our device, we have implemented a half-wavelength layered resonator in the axial direction, combined with a modification in the form of a protrusion on the back surface of the PZT transducer to also gain lateral control (see Fig. 1). In this way, we may control the trapping pattern of the manipulated particles in the lateral direction, simultaneously with keeping the trapped particles levitated and retained in the center of the fluid layer. As seen in Fig. 1, the
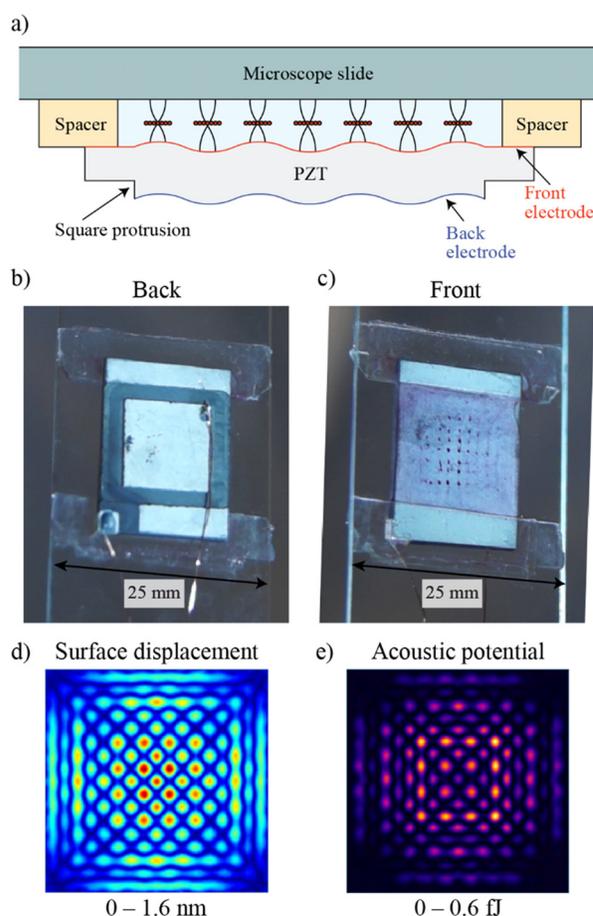
FIG. 1. (Color online) (a) Sketch of the device consisting of a strip electrode PZT transducer (gray), with a large front electrode (red) and a smaller back electrode (blue) on a square protrusion. It is attached to a microscope slide (teal) with double-sided adhesive tape (beige). Levitation and lateral trapping of suspended particles (red points) in the liquid (light blue) were provided by an array of acoustic potential minima set by the surface displacement of the PZT transducer. (b) Back-view showing the square-shaped protrusion (silver) in the center of the PZT transducer (blue-gray), the two slabs of adhesive tape (semi-transparent), and the microscope glass slide (transparent). (c) Front-view showing an array of trapped particles (red spots). (d) Color plot of the amplitude of the simulated surface displacement of the PZT transducer from 0 nm (blue) to 1.6 nm (red) on the front electrode. (e) Color plot of the simulated acoustic potential from 0 fJ (black) to 0.6 fJ (yellow), a pattern well-correlated to the displacement field.

1446   J. Acoust. Soc. Am. **149** (3), March 2021

Hammarström *et al.*
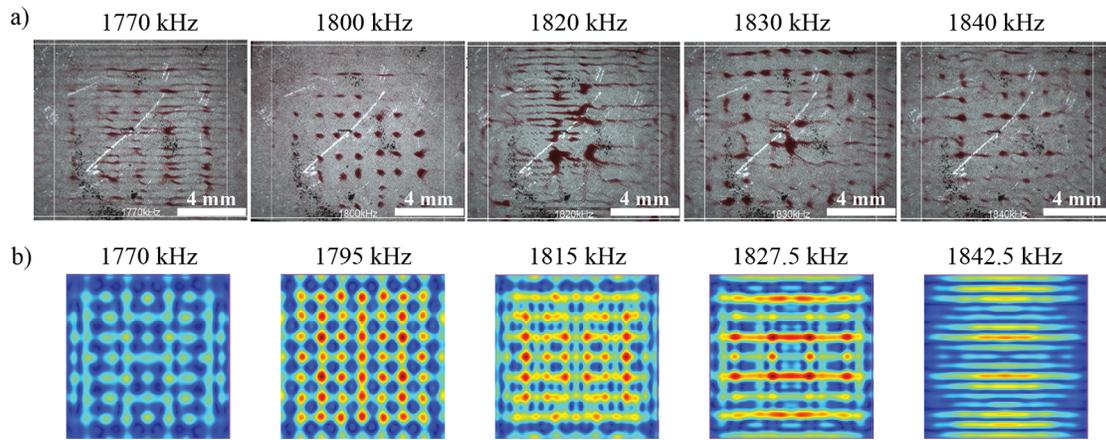
FIG. 2. (Color online) Manipulation of 10 μm particles at 4 V_{pp} enables fast manipulation in a wide frequency range. (a) Images are shown at 10 s after activation. As per design, 2D array of levitated acoustic traps occurs above the transducer at 1.8 MHz, and if the frequency is shifted to either side of the main mode, a variety of patterns emerge. (b) Qualitative prediction of these patterns is achieved by simulating the surface displacement of bulk modes in a free piezo element, where everything except the transducer protrusion is removed from the model. Aggregations at more frequencies are available in the supplementary material.[1]

acoustofluidic resonator is solely made from a piezo-ceramic plate, double-sided sticky tape, and a glass slide.

3D full-system simulations were performed for such a device by adaptation of the efficient numerical approach presented by Skov *et al.* (2019) that includes the piezoelectricity of the transducer; the solid mechanics of the transducer, the adhesive, and the glass; and the acoustics with viscous boundary layers in the water domain. Such simulations performed at 1.8 MHz showed that a modest removal by milling of only 10% of the piezoelectric material (specifically 100 μm of the 1020-μm-thick PZT transducer) around a 10×10 mm^2 square area on the back electrode, resulting in a $10 \times 10 \times 0.1$ mm^3 rectangular protrusion with an electrode, was sufficient to produce a regular horizontal array of force-potential minima in the fluid when driving the PZT transducer with an alternating current (ac)-voltage between the unmodified front-side electrode and the electrode left on the back-side protrusion. The model also suggested that such a geometry would localize the acoustic field to the region above the electrode where the electrical signal was applied and provide a regular array of stable points in the acoustic potential for particle levitation and lateral trapping in the mid-plane of the fluid. Crucially, it showed that the lateral force potential in the fluid was determined by the surface displacement of the PZT transducer in its specific bulk resonance modes. The pattern of this surface displacement field was also obtained in a reduced model containing only the PZT transducer. This simplification reduced the degrees of freedom of the simulation by 77% (i.e., from 1.3 to 0.3×10^6) and enabled characterization of resonance patterns for all frequencies in the range 1.76–1.84 MHz with 2.5 kHz resolution.

B. Trapping in a 2D array

As predicted by the simulation, a regular arrangement of levitated particles was obtained at 1.8 MHz. The central image in Fig. 2(a) shows this regular grid of 10-μm diameter particles achieved when using 4 V_{pp} amplitude. Around the central frequency, levitation could be maintained, but the lateral arrangement was less regular [Fig. 2(a)]. Drive frequencies in the range 1.73–1.84 MHz were evaluated, and each showed variations in trapping patterns during levitation for the above settings.[2] These patterns could be qualitatively reproduced by simulations of a free transducer protrusion where only the transducer parts were kept in the simulation. Shown in Fig. 2(b) are the simulated surface displacements looking at the strongest displacement mode in the respective sweep range.

Lower actuation voltages (2.3 V_{pp}) and smaller particles (3 μm) were also evaluated (Fig. 3), and under these conditions, the frequencies 1.78 and 1.80 MHz were shown to be the most effective trapping frequencies, and a more pronounced localization to the active area was visible. At these settings, a very low amount of input energy was required to achieve manipulation, especially at the central frequencies corresponding to the axial mode.
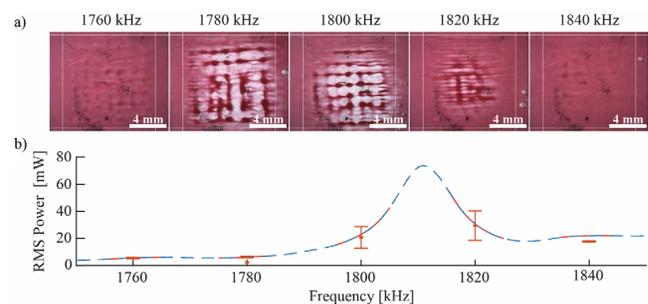
FIG. 3. (Color online) (a) The conformations of 3 μm beads show that the speed of lateral aggregation is different for the different frequencies, and images are shown after 180 s of aggregation at an applied voltage of 2.3 V_{pp}. (b) The corresponding RMS power is below 100 mW for all these patterns, and comparison with pattern formation shows that particularly efficient trapping is here achieved at 1780 and 1800 MHz. The electrical impedance of the transducer is available in the supplementary material.[1]

J. Acoust. Soc. Am. **149** (3), March 2021

Hammarström *et al.* 1447
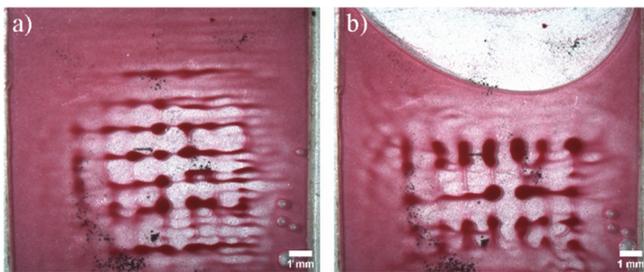
FIG. 4. (Color online) Since the grid-shaped lateral trapping pattern is defined locally in the transducer, the system is insensitive to changes in the fluid volume. Robust operation is here shown by comparing (a) the normal situation to (b) a situation where a large air-pocket (white region) is impinging on the trapping area. As a curved air-liquid interface cannot be used to support a standing wave, this comparison also shows that lateral resonances in the fluid volume are not important for the pattern formation. The captured particles are 3 μm polystyrene beads.

C. Robustness to bubbles and gas pockets

Removing the dependence on lateral resonances in the *fluid chamber* for 3D patterning significantly improves the operation robustness toward larger air bubbles in the fluid chamber. In conventional acoustofluidic devices, a standing wave has to be supported between reflecting surfaces in the fluid. However, as described in Sec. II A, in the proposed device, the trapping pattern arises from bulk modes in the PZT transducer and not from lateral resonances in the fluid chamber. This makes it insensitive to the presence of air-pockets in the fluid layer. Even in a device where a large air-pocket partially covers the transducer, particles will still be captured in the same arrangement as in a completely filled device where the sample is present (Fig. 4). Careful comparison of Figs. 4(a) and 4(b) shows that it is only the trapping sites closest to the bubble in Fig. 4(b) that are disturbed.

D. Dynamic control and coralling of particles

A large range of lateral modes is available within the levitation bandwidth (see Fig. 2). The matrix formation can therefore be changed on the fly by altering the drive frequency. It was found that the regularity of the particle matrix was improved by using a linear sweep in the driving frequency from 1.75 to 1.85 MHz with a sweep rate above 10 kHz. Interestingly, it was found that using very-low-

frequency sweep rates below 5 Hz allowed trapped sheets to physically move between the various modes contained in the sweep. If combining a low sweep rate with a slightly higher actuation voltage (5.6 V$_{pp}$), the particles could move between matrix nodes, and a corralled large centrally located sheet as shown in Fig. 5 could be created. Generally, when operating in this low sweep rate regime, the complete actuation-history was of importance for the emerging pattern, and an even larger variety of sheet patterns could be achieved by manual tuning of the frequency and amplitude. Randomly shifting the center frequency of low sweep rates was found to be an effective way of collecting the particles in the center of the trap referred to as mode hopping.

E. Medium exchange and washing

A common task in cell handling is to exchange the medium. This is done for a number of reasons, but typically in order to keep the cell medium fresh or to introduce different types of stains, fluorescent molecules, and chemical stimuli. It is shown in Fig. 6 how this operation can be performed *in situ*. The cells were initially corralled into a large sheet using mode hopping, and a piece of elastic tubing attached to a pump was held to the edge of the trap (picture in the supplementary material[1]). This was utilized instead of a pipette, as the flow rate could then be limited to 100 μl min^{-1} because of high fluid resistance. Introducing trypan blue along the top edge of the chamber and subsequently flowing clean medium allowed the introduction and removal of the stain to be performed on the levitated particles (video available in the supplementary material[1]). In about 1 min, the stain could be introduced and removed.

F. Arrays of levitated cells

The technology enables non-contact trapping and levitation of cell sheets in a 2D array formation (Fig. 7), potentially useful in 3D cell culture and tissue engineering applications. This was tested using a leukemia cell line (K562), fluorescently stained with the viability probe calcein green AM. By incubating the chamber with cell medium for 5 min (i.e., albumin-blocking) before introducing the cells with a pipette, unspecific binding to surfaces was minimized. Upon activation of the ultrasound the K562 cells formed levitated sheets analogous to those of the
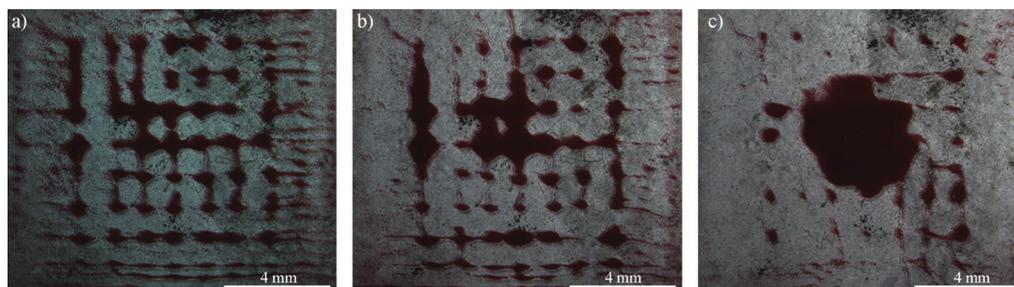
FIG. 5. (Color online) Images from a time-lapse taken over 1 min and 20 s, where frequency-hopping in a 100 kHz range from the central resonance is used to corral the particles into the center—forming one large thin levitated sheet. (a)–(c) Time-lapse images taken at 0, 36, and 72 s; the captured particles are 10 μm polystyrene beads.

FIG. 6. (Color online) A staining operation was performed on a trapped sheet where trypan blue is introduced along the top edge of the fluid cell and subsequently removed by flowing fresh medium from the same side. (a)–(c) Time-lapse images taken at 0, 40, and 80 s; the captured particles are $10\,\mu m$ polystyrene beads.

microspheres. This particular cell line is frequently used as a natural killer cell target and has a mean size of $17\,\mu m$ (Henslee *et al.*, 2011). It was found possible to arrange these cells in a series of levitated sheets arranged in a grid structure. Close inspection of the individual sheets indicated that a single layer of cells is formed in the peripheral regions and that a double layer is present in the center. This would indicate that the size of such a typical sheet in the array can be expected to be approximately 300–$400\,\mu m$ wide in the lateral dimensions but only about $30\,\mu m$ thick.

As the trapping system was capable of retaining the trapped aggregates against fluid flow, it was possible to generate heterogeneously structured sheets. To demonstrate this, two populations of K562 cells were labelled with two differently colored viability probes and sequentially introduced into the chamber. This produced aggregates where the core regions consisted of cells from the first population and the peripheral regions consisted of cells from the second population [Fig. 7(c)]. This result shows how a trapped cell aggregate can be spatially structured by sequential injection of cells. Combined with the corralling procedure shown with particles in Fig. 5, this method may be used in the future to produce a large co-culture biological membrane with a spotted structure.

G. Power consumption and battery operation

Since the modulus $|z_{pzt}|$ and the phase angle ϕ_{pzt} of the complex electrical impedance, z_{pzt}, of the transducer can easily be measured using an impedance analyzer, it is possible to calculate the root mean square (rms) or apparent power when applying the rms voltage v_{pzt},

$$p_{rms} = \left(v_{rms}^2/|z_{pzt}|\right)\cdot\cos\left(\phi_{pzt}\right). \tag{1}$$

As opposed to most acoustofluidic systems, the presented device requires no amplification circuitry to perform effective trapping but can be run directly from a function generator. If running a standard benchtop function generator at maximum output $10\,V_{pp}$ shared over the output impedance ($50\,\Omega$) and the transducer impedance (frequency-dependent), the total input power is between 20 and 220 mW, depending on the chosen frequency in our experiments (1.72–1.84 MHz). Within this frequency interval, successful trapping is realized, resulting in various particle patterns, as seen in Fig. 2. If lowering the voltage over the transducer to a constant $2.3\,V_{pp}$, the consumed power was lowered to 10–80 mW, but the range of relevant trapping frequencies was instead between 1.78 and 1.82 MHz. In conclusion, the device could be flexibly operated in the milliwatt power range and also displayed a trade-off between flexibility in terms of pattern formation and power consumption.

For the optimal frequency of 1.8 MHz, the lowest voltage that could levitate a $10\,\mu m$ polystyrene particle was found to be $231.1 \pm 27.6\,mV_{pp}$ ($n = 10$). At such a low voltage, the trapping device requires only $232.8 \pm 3.3\,\mu W$ of power to the transducer. This means that the system is capable of performing levitation also at sub-milliwatt powers.
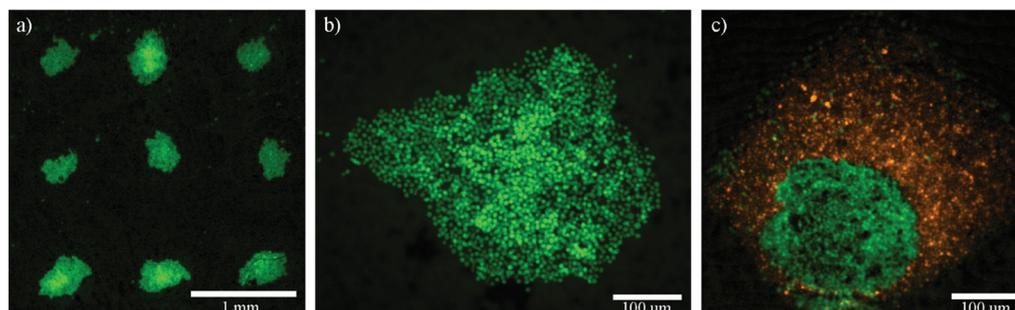
FIG. 7. (Color online) Fluorescence images of (a) an array of K562 cell sheets, a leukemia cell line, and (b) a close-up of a cell sheet. (c) Laterally heterogeneous constructs are possible by sequential injection. The fluorescent dyes used are viability probes (calcein green AM and calcein red orange) confirming that the cells remain viable in the trap.

J. Acoust. Soc. Am. **149** (3), March 2021

Hammarström *et al.* 1449

Due to the exceptionally low power consumption of the device, it was possible to consider entirely new driving circuitry for the transducer. To demonstrate a low-cost battery operated system, the traditional function generator, amplifier, and cooling systems were replaced by a digital clock generator set to create a 1.8 MHz square wave signal. A board containing the clock generator (Si5351) was available off the shelf and could be directly powered from a 3.6 V camera battery. As seen in Fig. 8, this setup was indeed able to levitate a matrix of trapped beads, and the total power drawn from the battery was measured at 77 mW, meaning that the acoustic trap could be powered for almost 2 days of the single battery. This shows the potential for a truly low-cost system, since the cost of the pre-made board was less than the price of the piezo, and with a custom design, the production costs would be marginal. Because of its simplicity and small size (cf. Fig. 8), the device can easily be put into a cell incubator or under a microscope without the need for any additional bulky external equipment.

III. DISCUSSION

A. Surface displacement of bulk modes

Acoustic trapping devices with the transducer inserted into the fluid layer have been used previously to enable efficient acoustic levitation. Much of the pioneering work by Bazou *et al.* (2005) and Coakley *et al.* (2004) utilized a system with a large disk-shaped transducer placed directly in the fluid. Furthermore, Evander *et al.* (2007), Johansson *et al.* (2013), and Lilliehorn *et al.* (2005b) have suggested the use of *miniaturized integrated transducers* (MITs), where a small transducer is also placed directly into the fluid channel. In relation to this, the primary advantage of the device presented herein is the level of lateral control that is easily obtained by selecting transducer and electrode dimensions where a 2D piezo surface vibration mode is coupled into the fluid and frequency matched with a mode for one-dimensional vertical levitation. Interestingly, these two modes seem to be decoupled in our device. In the axial

direction, a strong acoustic field is maintained over a wide range of frequencies, whereas the lateral modes are sensitive to smaller frequency changes. This allows flexible lateral manipulation while maintaining levitation. A highly interesting aspect of the lateral modes is that they stem from surface displacement of piezo modes and therefore depend on the material properties of the piezo material instead of the liquid, as is the case with the axial mode. This can be appreciated from Figs. 2(a) and 7(a), where the bead and cell clusters are separated by approximately 1 mm. This corresponds to a sound velocity of 3600 m/s when applying the $\lambda/2$-criterion at 1.8 MHz, which is reasonable for waves in the PZT-4D material but not in the fluid layer. This is also highlighted by the fact that array formation is maintained even in the presence of large air-pockets, such as in Fig. 4(b). To our knowledge, this is the first method that allows the length scales of the acoustic fields to be predictably selected in different directions. This occurs as the resonance of the axial field is dependent on the fluid material properties, while the lateral field depends on the mechanical properties of the piezo.

In trapping applications, the ability to form arrays of trapping minima in the acoustic potential is a tremendous advantage, as it allows screening combinations of two separate experimental parameters. In the case of MITs, a method for creating a grid of particles by inclusion of several ~1-mm-sized transducers (Lilliehorn *et al.*, 2005a) was suggested but only implemented along a single line and only demonstrated with trapped polymer beads. With the transducer dimensions presented herein (~1-cm-sized), we show the facile formation a larger-scale grid of trapped particles and cells using a single frequency and a single transducer. If the shape and size of the electrode were to be modified, it is likely that other patterns would emerge in the transducer in analogy with those formed on a regular Chladni plate (Wheatstone, 1833). We can thus view the transducer as a kind of miniaturized electromechanical Chladni plate.

A central finding in this study is that, even during levitation of particles in a plane about 0.2 mm above the piezo, the trapping pattern is determined by the displacement at the surface of the bulk mode in the piezo and not by lateral modes in the fluid, as is the classical scenario with a microchannel acting as a strongly reflecting 3D enclosure (Hagsäter *et al.*, 2007). This is supported by both the theoretical prediction of trapping patterns and the fact that a grid or array of trapped particles can be maintained despite the significant changes in boundary conditions, such as the impingement of a large air bubble (Fig. 4). In the case of MITs, a fine structure in the particle conformation above each integrated transducers was observed and previously attributed to near-field radiation effects, but with the new knowledge about the significance of surface displacement modes in the piezo layer, we can now better explain this pattern as shown in a supplementary simulation.[1] For the presented and future devices, this implies that a simulation of the isolated piezoelectric element is enough to predict what lateral distribution of trapping sites in the fluid will emerge
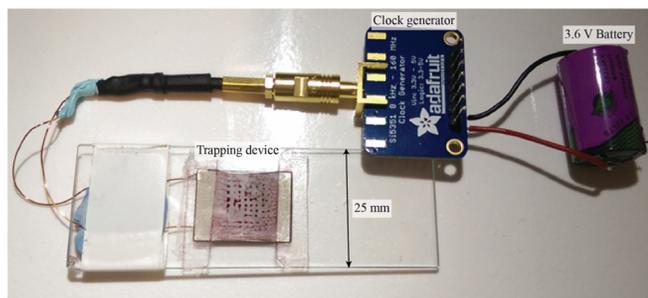
FIG. 8. (Color online) Low-power performance enables a battery operated low-cost device. Shown here is the trapping device performing acoustic levitation and arraying of 10 μm beads with actuation from a digital clock generator (blue chip). The clock generator is providing a digital 1.8 MHz signal, and the output is connected to the front and back of the PZT using two copper wires and an SMB-connector. The clock generator chip has a built-in voltage regulator and can therefore be powered directly from a 3.6 V battery as shown here.

1450   J. Acoust. Soc. Am. **149** (3), March 2021

Hammarström *et al.*

from a given transducer geometry, such that this geometry can be optimized beforehand to produce a desired pattern.

Removing the reliance of complex 3D cavity modes in the fluid has tremendous advantages when it comes to design freedom and robust operation. The usage of piezo modes for lateral manipulation means that the pattern is determined locally—decoupling it from the rest of the chip and the levitation mode. For instance, the fluidic system external to the transducer can be designed freely and flexibly, including a number of side channels and the usage of polymer materials without considering the acoustic absorption or poor reflection properties. It also suggests that several electrode elements could be put on a single large transducer if so desired. As shown by the experiment where a bubble impinges into the trapping site, it can also make the system more robust to changes, as the trapping is not determined by the system as a whole.

B. Fabrication advantages

Piezos with strip electrodes, where parts of the electrode are separated by superficial cuts, have been previously utilized for formation of a trapping grid by Neild *et al.* (2007). A related technique is used also in this work but now combined with levitation. In our simulations, a 2-mm-wide cut-depth corresponding to 10% of the material thickness was used, and this was found to induce lateral modes based on the electrode shape and not based on the entire piezoelectric slab. In previous acoustic trapping related works, a substantially deeper cut has been utilized in order to *remove* lateral modes (Hammarström *et al.*, 2014b). However, here we find that a very superficial cut is all that is required in order to *introduce* the new desired lateral modes. The use of patterned transducers enables further design freedom by localizing the effect to the modified electrode area and allowing piezos of arbitrary lateral dimensions to be used. A simulation contrasting the difference between an electrode patterned piezo and a piezo without this modification is provided in the supplementary material.[1] The use of strip electrodes enables rapid prototyping by greatly simplifying the fabrication process. Rather than using a scriber to manually cut the piezo into smaller pieces or working with uncured material, a sufficiently deep cut can be accomplished with micro milling. In our work, it was found that a 10% deep cut in the back side of the piezo layer is sufficient for controlling the surface displacement in the electrode area. This approach also allows the piezo material to be used as a lid for the fluid chamber without casting it in epoxy (or similar material) to extend the lateral dimensions. These circumstances make the fabrication process extremely simple: The device presented herein can namely be fabricated in less than 5 min by milling the pattern to the back side of the piezo and then simply taping it to a standard microscope slide.

C. Dynamic operation

Forming a grid or 2D array of trapping sites over a single transducer, instead of several small ones, has advantages when it comes to dynamic operation. Since the lateral modes are 2D and have a fundamental frequency that is much lower than that of the vertical mode (i.e., 1.8 MHz), a small change in frequency with respect to the vertical mode will still change the shape of the lateral field as seen through the particle conformations and in the simulations (Figs. 2 and 3 and supplementary material[1]). By jumping between these frequencies, the shape and position of the aggregates can be dynamically changed without losing the levitation function.

As shown in previous publications, frequency sweeps can be a powerful tool by enabling robustness to temperature changes and device variability (Vanherberghen *et al.*, 2010), flow-free transport of particles and cells (Manneberg *et al.*, 2009), and means for mechanically stimulating cells during culture (Jonnalagadda *et al.*, 2018). These approaches were also found to be applicable for controlling the surface displacement of the bulk mode used in this device. The demonstration included in this work shows how a slow and wide frequency sweep can be used to allow the particles to be merged into the central area of the trapping site.

If utilizing more advanced frequency selection schemes, it is likely that individual particles or cells could be moved in desired patterns either by methods such as suggested by Shaglwf *et al.* (2019) or Zhou *et al.* (2016). The potential advantage of utilizing this device with such methods is the ability to move cells and micro particles over cm-scale areas. In particular, the work by Zhou utilizes Chladni patterns that are analogues to the surface displacement of the bulk mode utilized in this device. By carefully designing the electrode size, and shape it is also possible that a more controlled and well-understood mode of mechanical stimulation can be made available, by for instance switching between two well-known patterns.

D. Large scale sheet formation

The final dimensions of the single sheet are approximately $4 \times 4\,mm^2$ in the experiments. In comparison to other acoustic-based methods for trapping and levitation, this is an extremely large structure. We anticipate that the size could be further increased by extending the size of the transducer or compounding several of them and that the formation of such large layers during levitation may prove useful for model systems of biological membranes (Tait *et al.*, 2019). In previous works by Tait *et al.*, acoustic trapping has been used to pre-culture a levitated sheet of epithelial cells. This was subsequently released onto a layer of fibroblasts, and after co-culture the layered membrane structure of a lung was successfully recapitulated. However, due to the small size of the final constructs, the ability to perform drug screening by probing either side of the membrane and effectively measure trans-epithelial electrical resistance (TEER) was limited. With some adaptation, the mechanism for lateral control presented herein might be able to produce significantly larger cell-constructs and, for instance, enable the use of microporous membrane supports for well plates

J. Acoust. Soc. Am. **149** (3), March 2021

Hammarström *et al.*　1451

E. Efficient conversion of power to trapping strength

Due to the removal of complex design criteria that typically follow acoustofluidic devices based on system resonances and cavity modes, the device could be designed as close as possible to an optimal one-dimensional (1D) layered resonator. Interestingly, the absence of a carrier layer has a positive impact on the energy density in the channel (Glynne-Jones et al., 2012). Because of this, using the piezo layer to form the base of the device (omitting carrier layers) provides a design with minimal power consumption. This is to our knowledge the first acoustofluidic trapping device capable of operation in the sub-milliwatt range. The power consumption is highly relevant if system cost and parallelization is considered. For instance, if the input power can be kept low, negligible heating is produced, and the need for cooling systems can be eliminated, reducing both cost and a potential source of failure. Furthermore, power amplifiers used for high voltage operation of piezoelectric elements, which are complex loads with typically low impedances, are difficult to design and costly. On the contrary, the device presented herein can be operated by a simple digital clock generator and battery powered, clearly showing the advantages of a low-power system. For sterility in cell culture applications, the removal of any wires going to and from the device is also of great practical importance, as the device can easily be moved from preparation in a laminar flow hood to an incubator in a closed box.

IV. MATERIALS AND METHODS

A. Device fabrication

A 2 MHz thickness mode PZT-4D piezo with the dimensions $22 \times 15 \times 1.02 \, \text{mm}^3$ was purchased with a pre-formed wrap gate (APC International, Ltd., Mackeyville, PA). A strip electrode pattern was milled into the back of the piezo with a 2 mm diamond coated drill bit (DATRON AG, Mühltal, Germany). As prescribed by the simulations, the back electrode was shaped into a $10 \times 10 \, \text{mm}^2$ square by cutting a path around it, as shown Fig. 1. The cut was 100 μm deep and possible to do in a single pass. Thereafter, wires were soldered to the wrap gate slot and directly on the back electrode.

The transducer was mounted on a microscope slide using two layers of tape (VHB F9460PC, 3M, Minneapolis, MN). The first tape layer had a thickness of 254 μm, and the second had a thickness of 127 μm, giving a combined thickness very close to 390 μm, as confirmed by optical microscopy. The tape pieces were placed on the short sides of the piezo such that an approximately $15 \times 15 \times 0.39 \, \text{mm}^3$ fluid cavity with two open sides was formed. The tape pieces were placed intentionally slanted to further disprove theories about lateral standing waves in the fluid.

B. Experimental

With the exception of the custom built clock generator circuit, the device was actuated directly from a benchtop function generator (DS345, Stanford Research Systems, Sunnyvale, CA). Fluids were added and removed from the open sides of the chip using a normal pipette. In the case of flow retention, the pipette was replaced with an elastic tube connected to a pump, and the chip was held at an angle such that the flow would go through the chip.

K562 cells were cultured under normal conditions in RPMI-1640 medium supplemented with 10% fetal bovine serum (FBS), 100 units ml^{-1} penicillin, and 100 μg ml^{-1} streptomycin, and this medium was also used to prefill the fluid cavity before loading the cells. Prior to loading, the cell culture was checked for viability and split into two populations and stained with the viability probes calcein green AM and calcein red orange, respectively.

Baudoin, M., Gerbedoen, J.-C., Riaud, A., Matar, O. B., Smagin, N., and Thomas, J.-L. (2019). "Folding a focalized acoustical vortex on a flat holographic transducer: Miniaturized selective acoustical tweezers," Sci. Adv. 5, eaav1967.

Bazou, D., Kuznetsova, L. A., and Coakley, W. T. (2005). "Physical enviroment of 2-D animal cell aggregates formed in a short pathlength ultrasound standing wave trap," Ultrasound Med. Biol. 31, 423–430.

Bouyer, C., Chen, P., Güven, S., Demirtaş, T. T., Nieland, T. J. F., Padilla, F., and Demirci, U. (2016). "A bio-acoustic levitational (BAL) assembly method for engineering of multilayered, 3D brain-like constructs, using human embryonic stem cell derived neuro-progenitors," Adv. Mater. 28, 161–167.

Burguillos, M. A., Magnusson, C., Nordin, M., Lenshof, A., Augustsson, P., Hansson, M. J., Elmér, E., Lilja, H., Brundin, P., Laurell, T., and Deierborg, T. (2013). "Microchannel acoustophoresis does not impact survival or function of microglia, leukocytes or tumor cells," PLoS One 8, e64233.

Caleap, M., and Drinkwater, B. W. (2014). "Acoustically trapped colloidal crystals that are reconfigurable in real time," Proc. Natl. Acad. Sci. U.S.A. 111, 6226–6230.

Chen, K., Wu, M., Guo, F., Li, P., Chan, C. Y., Mao, Z., Li, S., Ren, L., Zhang, R., and Huang, T. J. (2016). "Rapid formation of size-controllable multicellular spheroids via 3D acoustic tweezers," Lab Chip 16, 2636–2643.

Christakou, A. E., Ohlin, M., Önfelt, B., and Wiklund, M. (2015). "Ultrasonic three-dimensional on-chip cell culture for dynamic studies of tumor immune surveillance by natural killer cells," Lab Chip 15, 3222–3231.

Clark, C. P., Xu, K., Scott, O., Hickey, J., Tsuei, A.-C., Jackson, K., and Landers, J. P. (2019). "Acoustic trapping of sperm cells from mock sexual assault samples," Forensic Sci. Int. Genet. 41, 42–49.

Coakley, W., Bazou, D., Morgan, J., Foster, G., Archer, C., Powell, K., Borthwick, K. A., Twomey, C., and Bishop, J. (2004). "Cell–cell contact and membrane spreading in an ultrasound trap," Colloids Surf. B Biointerfaces 34, 221–230.

Courtney, C. R. P., Drinkwater, B. W., Demore, C. E. M., Cochran, S., Grinenko, A., and Wilcox, P. D. (**2013**). "Dexterous manipulation of microparticles using Bessel-function acoustic pressure fields," Appl. Phys. Lett. **102**, 123508.

Evander, M., Johansson, L., Lilliehorn, T., Piskur, J., Lindvall, M., Johansson, S., Almqvist, M., Laurell, T., and Nilsson, J. (**2007**). "Noninvasive acoustic cell trapping in a microfluidic perfusion system for online bioassays," Anal. Chem. **79**, 2984–2991.

Glynne-Jones, P., Boltryk, R. J., and Hill, M. (**2012a**). "Acoustofluidics 9: Modelling and applications of planar resonant devices for acoustic particle manipulation," Lab Chip **12**, 1417–1426.

Hagsäter, S. M., Jensen, T. G., Bruus, H., and Kutter, J. P. (**2007**). "Acoustic resonances in microfluidic chips: Full-image micro-PIV experiments and numerical simulations," Lab Chip **7**, 1336.

Hagsäter, S. M., Lenshof, A., Skafte-Pedersen, P., Kutter, J. P., Laurell, T., and Bruus, H. (**2008**). "Acoustic resonances in straight micro channels: Beyond the 1D-approximation," Lab Chip **8**, 1178–1184.

Hammarström, B., Nilson, B., Laurell, T., Nilsson, J., and Ekström, S. (**2014a**). "Acoustic trapping for bacteria identification in positive blood cultures with MALDI-TOF MS," Anal. Chem. **86**, 10560.

Hammarström, B., Evander, M., Wahlström, J., and Nilsson, J. (**2014b**). "Frequency tracking in acoustic trapping for improved performance stability and system surveillance," Lab Chip **14**, 1005.

Henslee, B. E., Morss, A., Hu, X., Lafyatis, G. P., and Lee, L. J. (**2011**). "Electroporation dependence on cell size: Optical tweezers study," Anal. Chem. **83**, 3998–4003.

Hultström, J., Manneberg, O., Dopf, K., Hertz, H. M., Brismar, H., and Wiklund, M. (**2007**). "Proliferation and viability of adherent cells manipulated by standing-wave ultrasound in a microfluidic chip," Ultrasound Med. Biol. **33**, 145–151.

Jing, P., Wu, J., Liu, G. W., Keeler, E. G., Pun, S. H., and Lin, L. Y. (**2016**). "Photonic crystal optical tweezers with high efficiency for live biological samples and viability characterization," Sci. Rep. **6**, 19924.

Johansson, L., Evander, M., Lilliehorn, T., Almqvist, M., Nilsson, J., Laurell, T., and Johansson, S. (**2013**). "Temperature and trapping characterization of an acoustic trap with miniaturized integrated transducers—towards in-trap temperature regulation," Ultrasonics **53**, 1020–1032.

Jonnalagadda, U. S., Hill, M., Messaoudi, W., Cook, R. B., Oreffo, R. O. C., Glynne-Jones, P., and Tare, R. S. (**2018**). "Acoustically modulated biomechanical stimulation for human cartilage tissue engineering," Lab Chip **18**, 473–485.

Krimholtz, R., Leedom, D. A., and Matthaei, G. L. (**1970**). "New equivalent circuits for elementary piezoelectric transducers," Electron. Lett. **6**, 398–399.

Lilliehorn, T., Nilsson, M., Simu, U., Johansson, S., Almqvist, M., Nilsson, J., and Laurell, T. (**2005a**). "Dynamic arraying of microbeads for bioassays in microfluidic channels," Sens. Actuators B Chem. **106**, 851–858.

Lilliehorn, T., Simu, U., Nilsson, M., Almqvist, M., Stepinski, T., Laurell, T., Nilsson, J., and Johansson, S. (**2005b**). "Trapping of microparticles in the near field of an ultrasonic transducer," Ultrasonics **43**, 293–303.

Manneberg, O., Vanherberghen, B., Önfelt, B., and Wiklund, M. (**2009**). "Flow-free transport of cells in microchannels by frequency-modulated ultrasound," Lab Chip **9**, 833.

Marzo, A., Seah, S. A., Drinkwater, B. W., Sahoo, D. R., Long, B., and Subramanian, S. (**2015**). "Holographic acoustic elements for manipulation of levitated objects," Nat. Commun. **6**, 8661.

Md Ali, M. A., Kayani, A. B. A., Yeo, L. Y., Chrimes, A. F., Ahmad, M. Z., Ostrikov, K. K., and Majlis, B. Y. (**2018**). "Microfluidic dielectrophoretic cell manipulation towards stable cell contact assemblies," Biomed. Microdevices **20**, 95.

Melde, K., Mark, A. G., Qiu, T., and Fischer, P. (**2016**). "Holograms for acoustics," Nature **537**, 518–522.

Neild, A., Oberti, S., Radziwill, G., and Dual, J. (**2007**). "Simultaneous positioning of cells into two-dimensional arrays using ultrasound," Biotechnol. Bioeng. **97**, 1335–1339.

Ohlsson, P., Petersson, K., Augustsson, P., and Laurell, T. (**2018**). "Acoustic impedance matched buffers enable separation of bacteria from blood cells at high cell concentrations," Sci. Rep. **8**, 9156.

Olofsson, K., Hammarström, B., and Wiklund, M. (**2018**). "Ultrasonic based tissue modelling and engineering," Micromachines **9**, 594.

Skov, N. R., Bach, J. S., Winckelmann, B. G., and Bruus, H. (**2019**). "3D modeling of acoustofluidics in a liquid-filled cavity including streaming, viscous boundary layers, surrounding solids, and a piezoelectric transducer," AIMS Math. **4**, 99–111.

Shaglwf, Z., Hammarström, B., Shona Laila, D., Hill, M., and Glynne-Jones, P. (**2019**). "Acoustofluidic particle steering," J. Acoust. Soc. Am. **145**, 945–955.

Tait, A., Glynne-Jones, P., Hill, A. R., Smart, D. E., Blume, C., Hammarstrom, B., Fisher, A. L., Grossel, M. C., Swindle, E. J., Hill, M., and Davies, D. E. (**2019**). "Engineering multi-layered tissue constructs using acoustic levitation," Sci. Rep. **9**, 9789.

Takebe, T., and Wells, J. M. (**2019**). "Organoids by design," Science **364**, 956–959.

Vanherberghen, B., Manneberg, O., Christakou, A., Frisk, T., Ohlin, M., Hertz, H. M., Önfelt, B., and Wiklund, M. (**2010**). "Ultrasound-controlled cell aggregation in a multi-well chip," Lab Chip **10**, 2727.

Voldman, J. (**2006**). "Electrical forces for microscale cell manipulation," Annu. Rev. Biomed. Eng. **8**, 425.

Wheatstone, C. (**1833**). "On the figures obtained by strewing sand on vibrating surfaces, commonly called acoustic figures," Philos. Trans. R. Soc. Lond. **123**, 593–633.

Zhou, Q., Sariola, V., Latifi, K., and Liimatainen, V. (**2016**). "Controlling the motion of multiple objects on a Chladni plate," Nat. Commun. **7**, 12764.

J. Acoust. Soc. Am. **149** (3), March 2021

Hammarström *et al.* 1453